forests

MDPI

Article

Effect of Climate on Carbon Storage Growth Models for Three Major Coniferous Plantations in China Based on National Forest Inventory Data

Lianjin Zhang [1], Guanghui Lai [2], Weisheng Zeng [3,*], Wentao Zou [4] and Shanjun Yi [5]

[1] Experimental Center of Forestry in North China, National Permanent Scientific Research Base for Warm Temperate Zone Forestry of Jiulong Mountain in Beijing, Chinese Academy of Forestry, Beijing 102300, China; zlianjin1102@126.com
[2] Beijing Municipal Forestry and Parks Planning and Resource Monitoring Center, Beijing Municipal Forestry Carbon Sinks and International Cooperation Affairs Center, Beijing 100029, China; laigh@126.com
[3] Academy of Forestry Inventory and Planning, National Forestry and Grassland Administration, Beijing 100714, China
[4] Research Institute of Forestry Policy and Information, Chinese Academy of Forestry, Beijing 100091, China; zouwt@caf.ac.cn
[5] Planning and Design Institute of Forest Products Industry, National Forestry and Grassland Administration, Beijing 100010, China; ysjyht@126.com
* Correspondence: zengweisheng0928@126.com

Abstract: Forest inventory data (FID) are important resources for understanding the dynamics of forest carbon cycling at regional and global scales. Developing carbon storage growth models and analyzing the difference and climate effect on carbon sequestration capacity have a great importance in practice, which can provide a decision-making basis for promoting high-quality development of forestry and implementing the carbon emission peak and carbon neutralization strategy. Based on the carbon storage dataset of 2680 sample plots from the ninth national forest inventory (NFI) of China, the carbon storage growth models and climate-sensitive variable-parameter carbon storage growth models for three major coniferous plantations (*Larix* spp., *Pinus massoniana*, and *Pinus tabuliformis*) were developed by using weighted nonlinear regression method. The effects of two climate factors (mean annual temperature (*MAT*) and mean annual precipitation (*MAP*)) on carbon storage growth and carbon sequestration capacity were analyzed and compared. The mean prediction error (*MPE*) of carbon storage growth models for three major coniferous plantations was less than 5%, and total relative error (*TRE*) was approximately less than 2% for self- and cross- validation. The maximum current annual increment of carbon storage for *P. massoniana*, *Larix*, and *P. tabuliformis* was 2.29, 1.89, and 1.19 t/(ha·a), respectively, and their corresponding age of inflection point was 9a, 14a, and 30a, respectively. The maximum average increment of carbon storage for *P. massoniana*, *Larix*, and *P. tabuliformis* was 1.85, 1.50, and 0.94 t/(ha·a), respectively, and their corresponding age of quantitative maturity was 16a, 24a, and 53a, respectively. The maximum average increment of carbon storage for the *P. massoniana* and *Larix* plantations was approximately 1.97 and 1.60 times, respectively, that of *P. tabuliformis* plantation. The average increment of carbon storage for the *P. massoniana* and *Larix* plantations reduced approximately by 4.5% and 3.8%, respectively, when the *MAT* decreases by 1 °C. The average increment of carbon storage for the *Larix* and *P. tabuliformis* plantations decreased by approximately 6.5% and 3.6%, respectively, when the *MAP* decreases by 100 mm. Our findings suggest that: the carbon sequestration capacity is from highest to lowest in the *P. massoniana*, *Larix*, and *P. tabuliformis* forests. *MAT* and *MAP* have different effects on the carbon growth process and carbon sequestration capacity of these plantations. The greatest impact on carbon sequestration capacity was detected in the *Larix* plantation, followed by the *P. massoniana* and *P. tabuliformis* plantations. It is essential to coordinate regional development and employ scientific management strategies to fully develop the maximum carbon sequestration capacity in terms of plantations in China. In the present study, we estimate the carbon storage in major coniferous plantations in China and describe a useful methodology for estimating forest carbon storage at regional and global levels.

Citation: Zhang, L.; Lai, G.; Zeng, W.; Zou, W.; Yi, S. Effect of Climate on Carbon Storage Growth Models for Three Major Coniferous Plantations in China Based on National Forest Inventory Data. *Forests* **2022**, *13*, 882. https://doi.org/10.3390/f13060882

Academic Editors: Ram P. Sharma and Xiangdong Lei

Received: 30 April 2022
Accepted: 2 June 2022
Published: 6 June 2022

Keywords: carbon storage; carbon sequestration capacity; variable parameter; growth model; climatic factor

1. Introduction

Forests, containing up to 80% and 40% of the terrestrial aboveground and belowground carbon (C), respectively, are among the most vital C pools on earth [1]. They also serve as a net C sink for atmospheric CO_2 [2]. Global forests will have huge carbon sequestration potential in the coming period [3]. Thus, forests play major roles in C cycling in terrestrial ecosystems [1,2,4–7].

Chinese forests cover most of the representative forest types in the Northern Hemisphere and function as a large C sink in the global C cycle [8,9]. C pools in Chinese forest ecosystems are dominantly attributed to those of vegetation and soil [10,11], and forest biomass (which only refers to tree biomass, i.e., excluding shrub and herb biomass) accounts for 55% of China's terrestrial vegetation biomass [12]. Chinese forests are young, have low average C density, and span large plantation areas, with lower C storage levels than other temperate forests worldwide [13,14]. Therefore, Chinese forests have great C sequestration potential [8,9,15]. Recently, the Central Committee of Communist Party of China has decided to integrate carbon emission peak and carbon neutralization into the overall layout of ecological civilization construction. Moreover, "Action Plan on Carbon Emission Peak Pre-2030" has been formulated to promote the action of carbon emission peak [16]. An essential aspect of achieving these goals on schedule is to improve the capacity of ecological carbon sink, strengthen land spatial planning and use control, and effectively play the role of carbon sequestration of forests, grasslands, wetlands, oceans, soils and permafrost. Thus, it is particularly important to assess and analyze carbon storage in forests, grasslands and wetlands using the comprehensive monitoring and evaluation results of national forest and grass ecosystem [16].

The accurate determination of carbon storage and carbon sequestration potential of forests at regional and national scales is popular for assessing the carbon budget of terrestrial ecosystem [8]. Forest biomass is the basis for calculating forest carbon storage and carbon sequestration potential. It is widely used to evaluate the patterns, processes and dynamics of C cycling in forest ecosystems at local, regional and global scales [17]. Therefore, extensive research was focused on estimating forest biomass and carbon storage worldwide on regional and national scales [9,17–24]. Large scale and continuous ground survey data play an extremely important role in estimating regional forest biomass or forest productivity. Moreover, forest inventory data (FID) are important resources for understanding the dynamics of forest biomass, net primary productivity (NPP), and carbon cycling at landscape and regional scales. Consequently, it is one of the important ways to estimate forest biomass, carbon storage and carbon sequestration potential at regional and national scales based on FID. Several studies have focused on estimating forest biomass and carbon storage based on FID at regional and national scales in China [9,17,18,20,23–30]. However, these studies were mostly performed more on a provincial scale, and less on a national scale. There is a lack of research on the dynamic changes of forest biomass and carbon storage in major plantation types on a national scale. In addition, forest carbon storage is affected by numerous factors, climate and stand age (or time since disturbance) are among the key drivers [13,31–39]. On the background of global change, the effects of climate change on forest carbon storage are very concerning [25,32–34]. Therefore, it is of great significance to establish dynamic forest carbon storage growth model at national level.

China is one of the countries with the largest planted forest areas in the world. The ninth national forest inventory (NFI) indicated that the total plantation area and stock volume were approximately 80,030,000 ha and 3,452,000,000 m^3, respectively. *Larix* spp., *Pinus massoniana*, and *Pinus tabuliformis* are China's main afforestation coniferous species and play important roles in wood production, carbon sequestration, and ecological services.

The total area and stock volume of these three tree species occupy 12.89% and 14.95% of which are planted, respectively [40]. FID is characterized by wide coverage, strong representation, detailed and accurate data, and diverse climate types, which makes it possible to develop carbon storage growth models for different forest types and analyze the differences in carbon sequestration capacity and the impact of climate factors. The objectives of the present study were: (1) to develop carbon storage growth models based on the FID for three major coniferous plantations in China, (2) to analyze the carbon growth process and carbon sequestration capacity of different plantations, and (3) to analyze and compare the effect of climate factors on carbon storage growth and carbon sequestration capacity. Our findings provide an estimation carbon storage of major plantations in China, a useful methodology for estimating forest carbon storage at regional and global levels, and a platform for promoting high-quality development of forestry and implementing the carbon emission peak and carbon neutralization strategy.

2. Materials and Methods

2.1. Data Collection and Processing

2.1.1. Forest Inventory Data

NFI of China has been conducted periodically (in five-year intervals) for more than 50 years. The ninth NFI (2014–2018) consists of 427,090 permanent plots distributed evenly across China. The investigations were carried out in accordance with the newest technical specifications on NFI [41]. The sample plots were square or rectangular, and their size varied between 0.06 and 0.08 ha [40].

The data sets used in this paper were collected from the ninth NFI. They consist of 2680 sample plots of the three major coniferous plantations, including 1080 of *Larix*, 820 of *P. massoniana,* and 780 of *P. tabuliformis* (Figure 1). Each sample plot included administrative sites, tree species, origin of forest, stand age, number, volume, biomass and carbon (stem, branches, leaves, roots and total) etc. Here, carbon storage is referred to the carbon stored in living tree biomass, including stems, branches, leaves and roots. The biomass and carbon stock of the stems, branches, leaves and roots of the sample tree were calculated based on the DBH of each sample tree, using the univariate tree biomass model and parameters for carbon accounting [42–45]. Next, the total carbon stock of the sample tree is calculated by adding that of the stem, branches, leaves and roots. In addition, the total carbon stock of sample plots was calculated by adding each sample tree, excluding the carbon of shrubs, grasses, and the carbon in dead wood, litter and soil. Finally, these data were converted into carbon stock per hectare according to the sample plot area. The statistical characteristics of modeling variables for three types plantations are listed in Table 1.

2.1.2. Climate Data

Several variables have been used to analyze the effects of climate change on forest biomass and carbon. The mean annual temperature (MAT) and mean annual precipitation (MAP) are among those commonly used [34–37,39,46]. In this study, we used the spatial Kriging method to derive MAT and MAP based on climatological data of the whole country from 1981 to 2015, geographical coordinates, and elevation of sample plots. Climatological data were downloaded from ClimateAP, an application for dynamic local downscaling of historical and future climate data in the Asia Pacific [47]. The descriptive characteristics of the climatic data in this study are presented in Table 1.

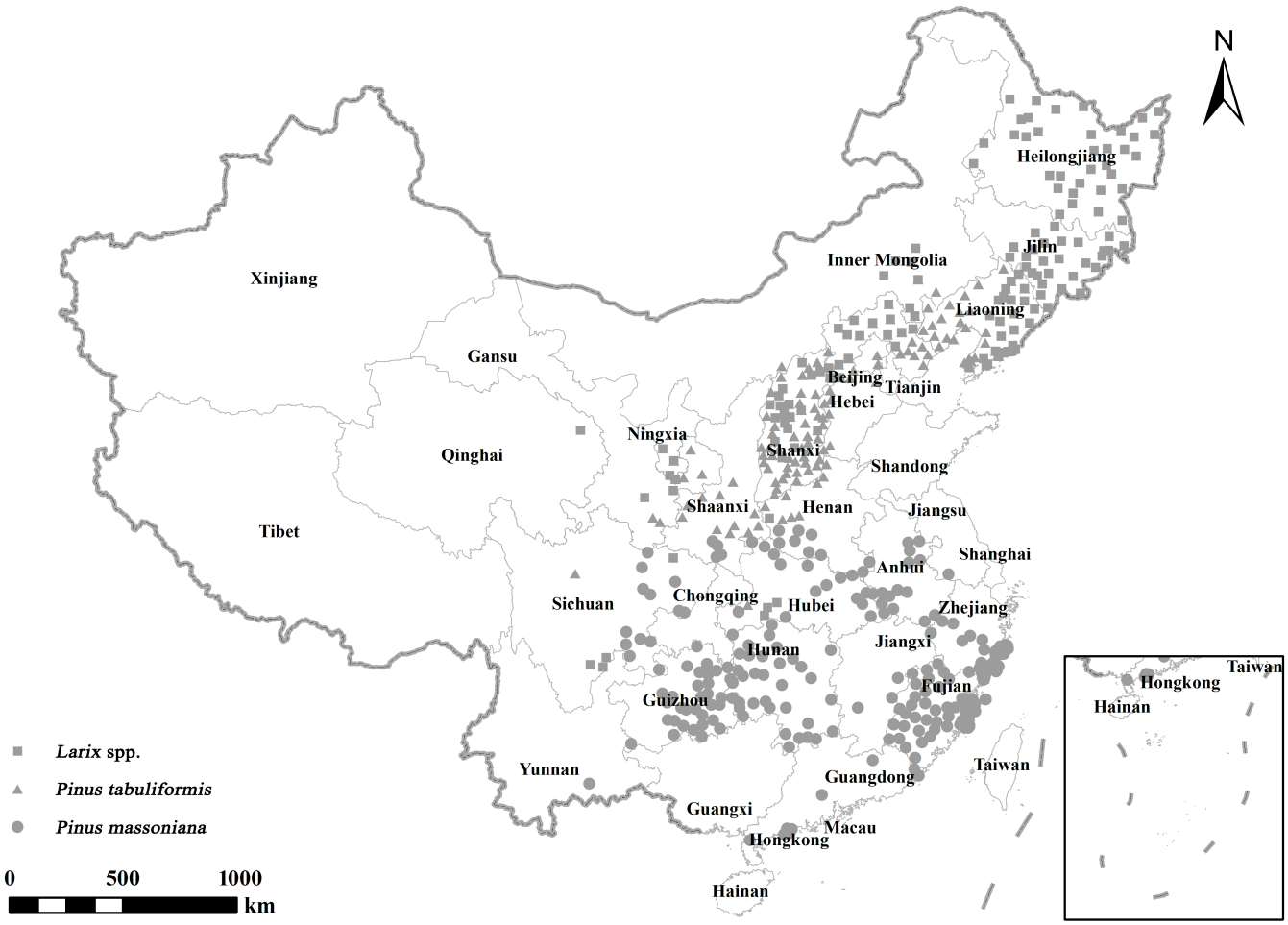

Figure 1. Location of sample plots in China.

Table 1. The statistical characteristics of modeling variables for three types of plantations.

Plantation Types	Variables	Min.	Max.	Mean	S.D.	C.V. (%)
Larix spp.	Carbon (t/ha)	0.10	129.20	33.80	25.60	75.90
	Mean annual precipitation (mm)	257	1223	569	194	34.12
	Mean annual temperature (°C)	0	15	7.5	2.8	38.02
	Age (a)	5	59	24.8	12.3	49.50
P. massoniana	Carbon (t/ha)	0.00	134.50	37.70	26.10	69.30
	Mean annual precipitation (mm)	740	2293	1338	328	24.51
	Mean annual temperature (°C)	12	20	16.5	2.0	12.22
	Age (a)	3	60	24.4	11.2	46.00
P. tabuliformis	Carbon (t/ha)	0.05	108.64	28.45	21.99	77.28
	Mean annual precipitation (mm)	297	1213	516	117	22.60
	Mean annual temperature (°C)	7	14	11.6	1.3	11.13
	Age (a)	3	68	33.2	13.1	39.50

2.2. Model Development

2.2.1. Basic Carbon Storage Growth Model

To date, thousands of biomass equations have been developed worldwide to accurately quantify forest biomass affected by carbon reduction and climate change [48]. However, most of these are allometric growth equations, and phenomenological growth equations are rarely used [49]. Phenomenological growth equations with biological significance are widely used in forest growth and harvest models. They reflect the changing law of biologi-

cal growth over time and theoretically predict biological growth that were not observed previously [50]. They belong to the category of mechanism model [51–54]. The Richards and Logistic growth equations, which are characteristics of the "S"-shaped curve, are most commonly used to describe tree growth development over time in application [55–57]. Carbon storage is usually expressed as a function of stand age in these two growth equations. Moreover, preliminary comparative analysis results also showed that these two growth equations were better than others. Therefore, the Richards and Logistic functions were considered as basic models from which to derive the carbon storage growth equations (Equations (1) and (2)).

$$C = a[1 - exp(-bA)]^c + \varepsilon \quad (1)$$

$$C = a/[1 + bexp(-cA)] + \varepsilon \quad (2)$$

where C is the stand carbon (t/ha), A is the stand age (a), a, b, c are the parameters to be estimated, and ε is the error term.

2.2.2. Climate-Sensitive, Variable-Parameter Carbon Storage Growth Model

Climatic variables were introduced to the basic carbon storage growth model using the variable-parameter method to analyze the impact of climate factors on carbon storage growth [58,59]. The parameters (a, b, c) in Equations (1) and (2) were expressed in terms of climate variables. Thus, we designed the climate-sensitive, variable-parameter carbon storage growth model using stand age and two climatic variables (Equations (3) and (4)):

$$C = (a_0 + a_1 \cdot MAP + a_2 \cdot MAT)\{1 - exp[-(b_0 + b_1 \cdot MAP + b_2 \cdot MAT)A]\}^{(c_0 + c_1 \cdot MAP + c_2 \cdot MAT)} + \varepsilon \quad (3)$$

$$C = (a_0 + a_1 \cdot MAP + a_2 \cdot MAT)/\{1 + (b_0 + b_1 \cdot MAP + b_2 \cdot MAT)exp[(c_0 + c_1 \cdot MAP + c_2 \cdot MAT)A]\} + \varepsilon \quad (4)$$

where a_0, b_0, c_0 are fixed parameters, a_1, b_1, c_1 are variable parameters of MAP, a_2, b_2, c_2 are variable parameters of MAT, and the other variables are the same as those described above.

The four carbon storage growth equations (Equations (1)–(4)) were fitted using the nonlinear weighted regression method [60,61]. Weighted regression was used to eliminate heteroscedasticity. The weight function of each model was determined from the regression equation fitted independently by OLS. Two sides of the equations were multiplied by the weight factor $w = 1/A$, when ForStat v.2.2 (Tang S.Z., Beijing, China) was used to estimate the parameters by the two-stage error-in-variable modeling method [60,61].

2.3. Model Evaluation and Comparison

Four statistical criteria were used for model evaluation and comparison: coefficient of determination (R^2), root mean square error ($RMSE$), total relative error (TRE), and mean prediction error (MPE), as shown in Equations (5)–(8) [34,60].

$$R^2 = 1 - \sum_{i=1}^{n}(C_i - \hat{C}_i)^2 / \sum_{i=1}^{n}(C_i - \overline{C})^2 \quad (5)$$

$$RMSE = \sqrt{\sum_{i=1}^{n}(C_i - \hat{C}_i)^2/(n-p)} \quad (6)$$

$$TRE = 100 \times \sum_{i=1}^{n}(C_i - \hat{C}_i)^2 / \sum_{i=1}^{n}\hat{C}_i \quad (7)$$

$$MPE = 100 \times t_\alpha \times \left(RMSE/\overline{C}\right)/\sqrt{n} \quad (8)$$

where C_i are observed values, $\hat{C}_i$ are estimated values, $\overline{C}$ is mean value of samples, n is the number of samples, p is the number of parameters, and t_α is the t value at confidence level α with $n - p$ degrees of freedom.

2.4. Inflection Point Age of Model

According to the characteristics of the carbon storage growth equations, the inflection point age of Equations (1) and (2), also known as the age with the maximum current annual increment, can be described as Equations (9) and (10), respectively.

$$A^* = (1/b) \times ln(c) \quad (9)$$

$$A^* = (1/c) \times ln(b) \quad (10)$$

where A^* is the age of inflection point, and the other variables are the same as those described above.

3. Results

3.1. Fitting and Comparisons for Stand Carbon Storage Growth Model

Two carbon storage growth models were used as candidate base models (Table 2). The data from all sample plots (1080 for *Larix*, 820 for *P. massoniana*, and 780 for *P. tabuliformis*) were used to fit the base models. Parameter estimates and fitting statistics indices of carbon storage growth model (Equations (1) and (2)) for three plantation types are shown in Table 2. The results show that both equations fit the stand carbon growth well, with the absolute value of $MPE < 5\%$ and $TRE < 5\%$. Furthermore, the root mean square error ($RMSE$) for both equations are relatively small, fluctuating around 20 t·ha^{-1}. However, the coefficient of determination (R^2) for both equations are relatively low, ranging from 0.254 to 0.423. According to the fitting effect of three plantation types (Figures 2–4), both equations can objectively reflect the average growth process of carbon (Figure 5). The Equation (1) was clearly better than Equation (2) fitting the stand carbon growth, especially with the difference of TRE being more obvious (Table 2). Equation (1) was further analyzed by evaluating its predictive ability using the five-fold cross-validation technique. There was almost no difference in TRE between the five-fold cross-validation and the total, indicating that Equation (1) is of good stability and prediction ability. Therefore, Equation (1) in Table 2 was selected as the best base model.

Table 2. Parameter estimates and fitting statistics indices of base model.

Plantation Types	Models	Parameter Estimates			Fitting Statistics Indices			
		a	*b*	*c*	R^2	*RMSE*	*MPE*	*TRE*
Larix spp.	Equation (1)	66.1141	0.05953	2.2248	0.420	19.55	3.47	0.56
	Equation (2)	51.0975	19.3295	0.1663	0.391	20.02	3.56	2.73
P. massoniana	Equation (1)	55.4460	0.08363	2.0604	0.287	22.08	4.05	0.96
	Equation (2)	45.5767	18.1671	0.2296	0.254	22.59	4.14	4.04
P. tabuliformis	Equation (1)	91.0381	0.02726	2.2340	0.423	16.73	4.13	0.00
	Equation (2)	48.6158	35.8971	0.1216	0.409	16.92	4.17	0.85

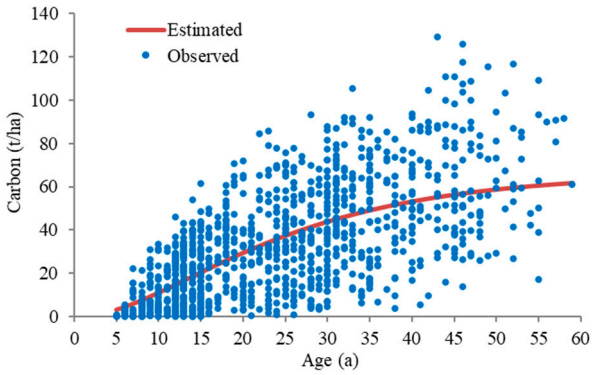

Figure 2. The fitting effect of carbon growth in the *Larix* plantation.

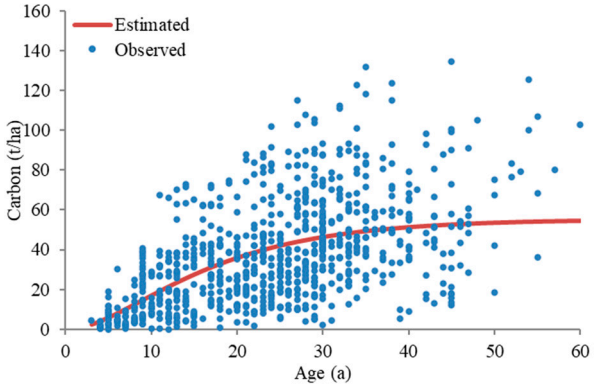

Figure 3. The fitting effect of carbon growth in the *P. massoniana* plantation.

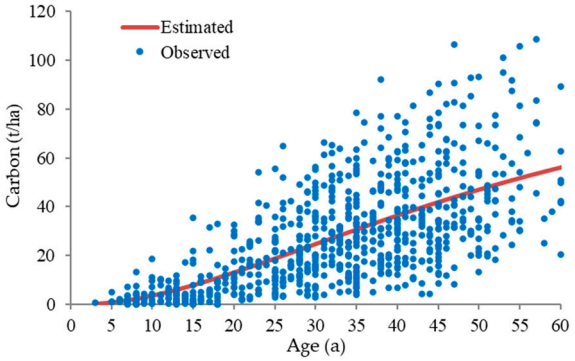

Figure 4. The fitting effect of carbon growth in the *P. tabuliformis* plantation.

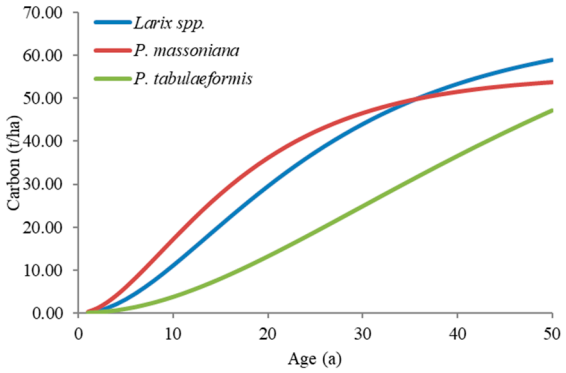

Figure 5. The average growth process of carbon storage for the three plantations.

3.2. Climate-Sensitive, Variable-Parameter Carbon Storage Growth Model

The two climatic variables (MAT and MAP) were introduced into each parameter of the basic carbon storage growth model (Equation (1)) in linear form. Thus, the climate-sensitive, variable-parameter carbon storage growth model (Equation (3)) was obtained. The complete data for each tree species were used to fit the Equation (3). Parameter estimates and fitting statistics indices of Equation (3) for the three plantation types are listed in Tables 3 and 4, respectively. The MAP for the *Larix* plantation has significant impact on the three parameters (a, b, c), while the MAT has significant impact on parameters of asymptote (a) and rate (b) (Table 3). Table 3 also shows that MAT and MAP had no significant effect on most parameters of the *P. massoniana* plantation, and that only MAT had a significant effect on shape parameter (c). Furthermore, MAP had a significant effect on the three parameters (a, b, c) of the *P. tabuliformis* plantation, whereas MAT had no significant effect on these three parameters (Table 3).

Table 3. Parameter estimates of Model (3).

Plantation Types	Constant Parameters			Variable Parameters					
	a_0	b_0	c_0	a_1	a_2	b_1	b_2	c_1	c_2
Larix spp.	69.0409	0.0000	0.0000	−40.9762	28.3544	0.1943	−0.04374	5.2510	0.0000
P. massoniana	53.1713	0.1070	8.6018	0.0000	0.0000	0.0000	0.0000	0.0000	−0.3353
P. tabuliformis	131.8019	0.01216	2.0412	−30.3743	0.0000	0.01614	0.0000	−0.07820	0.0000

Table 4. Fitting statistics indices of Model (3).

Plantation Types	Fitting Statistics Indices			
	R^2	*RMSE*	*MPE*	*TRE*
Larix spp.	0.469	18.72	3.34	1.14
P. massoniana	0.293	22.01	4.04	1.10
P. tabuliformis	0.438	16.54	4.08	−0.06

The fitting statistics indices of Equation (3) (Table 4) showed that most of the fitting statistics indices for the three plantation types were improved except for the slight increase of TRE. This finding indicated that a substantial proportion of the stand carbon variations was better explained by the effects of the age and climatic variables (MAT and MAP) than the effect of age alone (Table 4).

3.3. Carbon Sequestration Capacity of the Three Plantations Types

The current annual and average increment of carbon storage curves for the three plantations types were generated according to Equation (1) and its parameter estimates (Table 2) (Figures 6 and 7). And the ages of inflection point and quantitative maturity for the three plantations types are listed in Tables 5 and 6, respectively. It showed that the inflection point age for *Larix*, *P. massoniana*, and *P. tabuliformis* was 14a, 9a, and 30a, respectively, and their corresponding maximum current annual increment of carbon storage were 1.89, 2.29, and 1.19 t/(ha·a), respectively (Table 5). The age of quantitative maturity for *Larix*, *P. massoniana*, and *P. tabuliformis* was 24a, 16a, and 53a, respectively (Table 6), and their corresponding maximum average increment of carbon storage was 1.50, 1.85, and 0.94 t/(ha·a), respectively (Figure 7). In the present study, the maximum average increment of carbon storage was taken as the basis for comparison to reflect carbon sequestration capacity. Thus, the carbon sequestration capacity is highest to lowest in the *P. massoniana*, *Larix*, and *P. tabuliformis* forests. Moreover, the carbon sequestration capacity of the *P. massoniana* and *Larix* forests is approximately 1.97 and 1.60 times, respectively, that of the *P. tabuliformis* forest. The difference in average increment of carbon storage among different plantations types gradually decreased with increasing forest age (Table 6 and Figure 7). These results indicate that the carbon sequestration capacity of different plantations types varies greatly, and that each plantation type has its reasonable management cycle. In order to fully develop the maximum production potential in terms of plantation in China, it is vital to coordinate regional development and implement scientific management strategies to fully develop the maximum production potential of plantations in China.

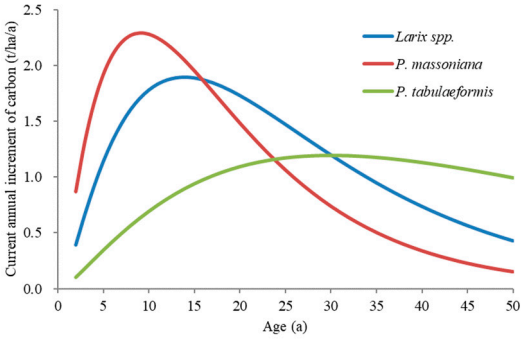

Figure 6. Current annual increment of carbon storage curves for the three plantation types.

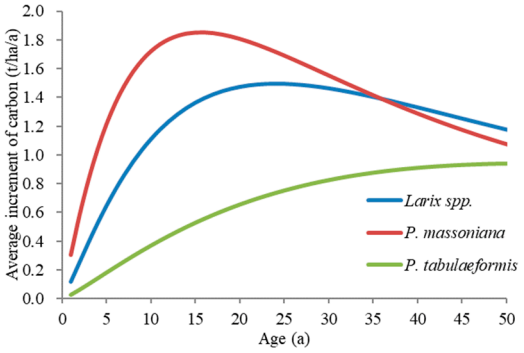

Figure 7. Average increment of carbon storage curves for the three plantation types.

Table 5. Comparison of current annual increment of carbon storage on age of inflection point for three plantation types.

Plantation Types	Age of Inflection Point(a)	Maximum Current Annual Increment of Carbon (t/(ha·a))
Larix spp.	14	1.89
P. massoniana	9	2.29
P. tabuliformis	30	1.19

Table 6. Comparison of average increment of carbon storage on different ages among the three plantation types.

Plantation Types	Average Increment of Carbon (t/(ha·a))					
	5	**10**	**15**	**20**	**25**	**Max.**
Larix spp.	0.65	1.11	1.37	1.48	1.50	1.50
P. massoniana	1.21	1.72	1.85	1.81	1.69	1.85
P. tabuliformis	0.18	0.37	0.53	0.66	0.75	0.94

3.4. Effect of Climate on Carbon Sequestration Capacity in the Three Plantation Types

According to Equation (3) and its parameter estimates (Table 3), the carbon growth process of the three plantation types were affected by the climatic variables (*MAT* and *MAP*) in varying degree.

3.4.1. *Larix* spp. Plantation

MAT and *MAP* had significant effects on the carbon growth process of *Larix* plantation, however, they share a complex relationship (Table 3). Nine climate scenarios, including high-temperature (15 °C), middle-temperature (7.5 °C), low-temperature (0 °C), more-precipitation (1220 mm), middle-precipitation (735 mm) and less-precipitation (250 mm),

were generated according to the range of *MAT* and *MAP* of *Larix* sample plots in Table 1. Except for high-temperature and less-precipitation (which had no solution due to the parameters of this model exceeding the reasonable range), the carbon growth characteristics of the other eight climate scenarios are shown in Table 7.

Table 7. Comparison of carbon growth characteristics of different climate scenarios for three plantation types.

Plantation Types	Climate Scenarios	Age of Inflection Point (a)	Maximum Current Annual Increment of Carbon (t/(ha·a))	Age of Quantitative Maturity (a)	Maximum Average Increment of Carbon (t/(ha·a))
Larix spp.	High-temperature and more-precipitation (CS-I)	11	4.20	18	2.54
	High-temperature and middle-precipitation (CS-II)	18	2.67	30	1.82
	Middle-temperature and more-precipitation (CS-III)	10	3.27	15	1.98
	Middle-temperature and middle-precipitation (CS-IV)	13	2.81	21	1.92
	Middle-temperature and less-precipitation (CS-V)	18	0.87	33	0.74
	Low-temperature and more-precipitation (CS-VI)	8	1.79	13	1.08
	Low-temperature and middle-precipitation (CS-VII)	10	2.36	16	1.61
	Low-temperature and less-precipitation (CS-VIII)	6	1.82	11	1.68
P. massoniana	Low-temperature (CS-IX)	15	2.35	24	1.54
	Middle-temperature (CS-X)	11	2.48	19	1.78
	High-temperature (CS-XI)	6	2.90	11	2.40
P. tabuliformis	Less-precipitation (CS-XII)	42	1.04	75	0.84
	Middle- precipitation (CS-XIII)	29	1.33	51	1.08
	More- precipitation (CS-XIV)	22	1.52	38	1.25

The age of inflection point and quantitative maturity for eight climate scenarios ranged from 6a to 18a and from 11a to 33a, respectively. The minimum and maximum values of these two age types were in the climate scenario of CS-V and CS-I, respectively (Table 7). Moreover, the maximum current annual and average increment of carbon storage of eight climate scenarios was between 0.87 and 4.20 t/(ha·a), and between 0.74 and 2.54 t/(ha·a), respectively. The maximum and minimum values of these two types of carbon growth were also in the climate scenario of CS-I and CS-V, respectively (Table 7). In addition, the top three climate scenarios with the largest average increment of carbon storage were CS-I, CS-III, and CS-IV, with a corresponding average increment of carbon storage of 2.54, 1.98, and 1.92 t/(ha·a), respectively, and the corresponding quantitative maturity ages of 18a, 15a, and 21a, respectively (Table 7). Furthermore, the age of quantitative maturity increased with the increase in temperature both under conditions of more or middle precipitation. The carbon sequestration capacity of *Larix* plantation increased with the increase in temperature under more precipitation conditions (Figure 8), but increased first, then decreased with the increase in temperature under middle precipitation conditions (Table 7). Moreover, the carbon sequestration capacity of *Larix* plantation increased with the increase of precipitation under high and middle temperature conditions, whereas the age of quantitative maturity decreased. Conversely, both the carbon sequestration capacity increased first, then decreased with the increase of precipitation under low temperature condition (Table 7). Finally, the maximum average increment of carbon storage of these three climate scenarios under middle temperature was 1.98, 1.92, and 0.74 t/(ha·a), respectively (Table 7). Taking

these data as the standard for measuring the carbon sequestration capacity, we determined that, when *MAP* reduced from 1220 to 250 mm, the corresponding carbon sequestration capacity will be reduced by 63%. It is equivalent to the average carbon sequestration capacity reduced by approximately 6.5% for every 100 mm decrease in *MAP*. The maximum average increment of carbon storage of the three climate scenarios under more precipitation was 2.54, 1.98, and 1.08 t/(ha·a), respectively (Table 7 and Figure 8). Taking these data as the standard to measure the carbon sequestration capacity, we found that, when *MAT* reduced from 15 °C to 0 °C, the corresponding carbon sequestration capacity will be reduced by 57%. This value is equivalent to the average carbon sequestration capacity reduced by about 3.8% for every 1 °C decrease in *MAT*.

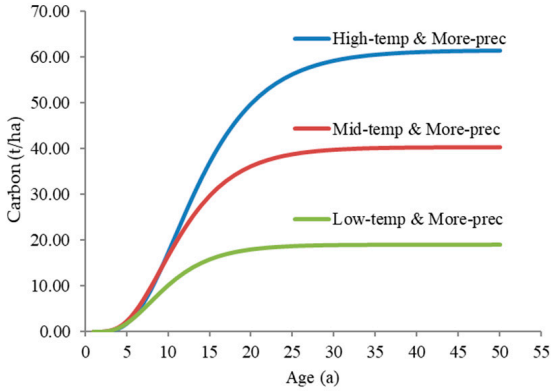

Figure 8. Growing process of carbon storage in *Larix* plantation under three climate scenarios.

3.4.2. *P. massoniana* Plantation

The carbon growth process of *P. massoniana* plantation was not significantly affected by *MAP*, but significantly affected by *MAT*, and the carbon sequestration capacity increased with the increase in temperature (Table 3). Based on the range of *MAT* in *P. massoniana* sample plots (Table 1), three climate scenarios, including low-temperature (12 °C), middle-temperature (16 °C), and high-temperature (20 °C), were generated. The carbon growth characteristics of the three climate scenarios are shown in Table 7.

The ages of inflection point and quantitative maturity for the three climate scenarios were between 6a and 15a, and between 11a and 24a, respectively (Table 7). Moreover, the corresponding ages all decreased with the increase in temperature. The maximum current annual and average increment of carbon storage for the three climate scenarios ranged from 2.35 to 2.90 t/(ha·a), and from 1.54 to 2.40 t/(ha·a), respectively (Table 7). The corresponding carbon growth all increased with the increase in temperature (Table 7 and Figure 9). Furthermore, taking mean carbon growth as the standard to measure the carbon sequestration capacity, we found that, when *MAT* increased from 12 °C to 20 °C, the corresponding carbon sequestration capacity will be enhanced by 56%. This value is equivalent to the average carbon sequestration capacity being enhanced by approximately 7.0% for every 1 °C increase in *MAT*. Conversely, when *MAT* reduced from 20 °C to 12 °C, the corresponding carbon sequestration capacity will be decreased by 36%. This value is equivalent to the average carbon sequestration capacity being decreased by approximately 4.5% for every 1 °C decrease in *MAT*.

3.4.3. *P. tabuliformis* Plantation

The carbon growth process of *P. tabuliformis* plantation was not significantly affected by *MAT* but significantly affected by *MAP*, and the carbon sequestration capacity increased with the increase in precipitation (Table 3). Based on the range of *MAP* for *P. tabuliformis* sample plots in Table 1, three climate scenarios, including more-precipitation (1200 mm), middle-precipitation (750 mm), and less-precipitation (300 mm), were generated. The carbon growth characteristics of three climate scenarios are listed in Table 7.

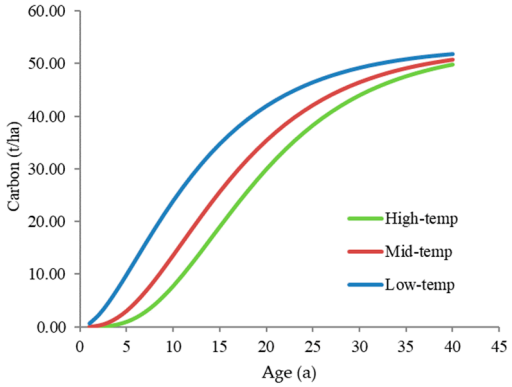

Figure 9. Growing process of carbon storage in *P. massoniana* plantation under three climate scenarios.

The age of inflection point and quantitative maturity for the three climate scenarios ranged from 22a to 42a, and from 38a to 75a, respectively (Table 7). Moreover, the corresponding ages all decreased with the increase in precipitation. This finding also showed that the maximum current annual and average increment of carbon storage of three climate scenarios changed between 1.04 and 1.52 t/(ha·a), and between 0.84 and 1.25 t/(ha·a), respectively (Table 7). The corresponding carbon growth all increased with the increase in precipitation (Table 7 and Figure 10). In addition, taking mean carbon growth as the standard for measuring the carbon sequestration capacity, when *MAP* increased from 300 to 1200 mm, the corresponding carbon sequestration capacity will be enhanced by 49%. This value is equivalent to the average carbon sequestration capacity being enhanced by approximately 5.4% for every 100 mm increase in *MAP*. Conversely, when *MAP* reduced from 1200 to 300 mm, the corresponding carbon sequestration capacity will be decreased by 33%. This value is equivalent to the average carbon sequestration capacity being reduced by about 3.6% for every 100 mm decrease in *MAP*.

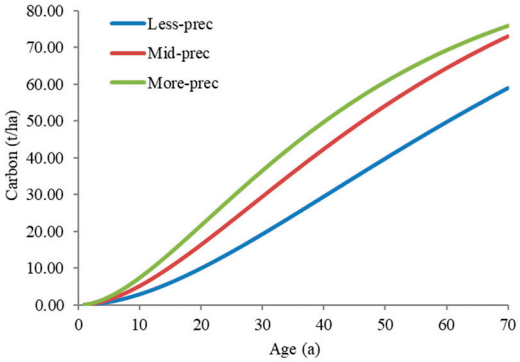

Figure 10. Growing process of carbon storage in *P. tabuliformis* plantation under three climate scenarios.

4. Discussion

4.1. Performance of Carbon Storage Growth Models

This study provided an effective set of model tools to estimate stand carbon storage growth in the three major species plantations in China at national scales. These tools can be used to estimate carbon storage growth based on FID. Some stand variables, including age, average diameter at breast height (Dg), basal area (BA), density (N), mean height (H) and volume (V), are typically introduced into carbon models [19–21,29,31,33,35,36]. Most of these equations are allometric growth equations, as phenomenological growth equations are rarely used [24]. Two phenomenological growth equations, where carbon storage is only expressed as a function of stand age, were developed in the present study. However, accurately estimating stand carbon storage only from age is difficult at national scales [32,35–37]. Climatic factors are also good predictors for stand carbon storage [32,35].

Thus, the Equations (1) and (2) were established using age only, and Equations (3) and (4) were set up with the introduction of MAT and MAP. It was showed that Equations (1) and (2) fit the stand carbon growth well, with the absolute value of MPE < 5% and TRE < 5%. The root mean square error ($RMSE$) for both equations was relatively small, fluctuating at approximately 20.00 t·ha^{-1}. However, Equation (1) had better prediction qualities than Equation (2). Therefore, Equation (1) was selected as the best base model. Equation (3) produced more accurate estimates than Equation (1) for the stand carbon growth based on decreasing $RMSE$ and MPE, as well as increasing R^2. This finding was supported by other stand growth models [25,34–39].

It should be noted that the coefficient of determination (R^2) for equations was low due to the approach of substituting spatial differences for time differences, which is also a normal phenomenon. The primary purpose of this research was to accurately evaluate the difference in carbon sequestration capacity for different types of plantations and their response to climatic factors at a national scale. Therefore, it was not necessary to accurately simulate carbon growth under different site conditions. Our work showed that MPE and TRE of all carbon storage growth models were less than 5% and 3%, respectively (Tables 2 and 4), indicating that the fitting effect is acceptable. If the carbon storage growth models are developed using the average values of sample plots at the same stand age, the range of R^2 for these models will increase from 0.174–0.420 to 0.721–0.889. Obviously, such models are inconsistent with our primary research purpose, and their results would not objectively and comprehensively reflect the overall actual carbon storage. Moreover, almost all the sample plots data of the three plantations for NFI in China were used for modelling, these data are sufficiently representative of the average carbon storage growth of real stands and can objectively reflect the actual carbon storage and the differences among different plantation types.

Of course, we have to acknowledge that the approach used in this study has its own limitation. However, this approach assumed that the stands of certain plantation type with different ages which are located on different sites can represent the growth process of the same stand with different ages on average site condition. Based on the central limit theorem, it should be able to reflect the average state when the number of modeling samples is large enough. Datasets of sample plots in this study were from the ninth NFI of China, widely distributed all over the country, and almost all sample plots of the three plantation types were used for modelling. Obviously, these data can meet the hypothetical condition. In other words, we can assume that NFI data-based models can objectively represent real state of carbon storage and average difference among plantation types.

4.2. Climate Effects on Carbon Storage Growth Models

It is very important to grasp the impact of climate change on carbon storage to implement national strategic decision. Climate can modify the carbon storage growth process of individual trees and subsequently affect carbon storage at whole stand and large scales. In previous studies, many seasonal and annual climate factors, including precipitation of the wettest quarter (mm), precipitation of total growing season (mm), MAP, MAT, mean monthly temperature (°C), mean temperature of growing season (°C), mean temperature of the wettest quarter (°C), and mean temperature of the driest quarter (°C), have been introduced into the biomass and carbon storage models [25,26,33–36,46,62,63].

The relationship between stand carbon storage and climatic factors must be known to illustrate the effects of climate change on stand carbon storage growth [33,35]. Given that carbon storage is affected by climatic factors [25,32,35], and that climatic factors affect the parameters of carbon storage models, a carbon storage model that considers climate effects is theoretically better. Thus, we developed climate-sensitive, variable-parameter carbon storage growth models (Equation (3) and Table 2) with the introduction of climatic factors (MAT and MAP). This study shown that the carbon storage growth model that considers climate effects had better performance than the basic models. Our findings showed that the carbon storage growth model that considered climatic factors (MAT and

MAP) performed better than the basic models. Furthermore, the present study confirmed the significant effects of climatic factors (*MAT* and *MAP*) on the process of stand carbon storage growth. This result is consistent with that of previous studies, which reported that the introduction of climatic factors improved the performance of carbon storage models [35]. Previous research also highlighted the important role of temperature and precipitation in tree growth. *MAT* and *MAP* were often used to analyze the climate effect on tree biomass and carbon storage due to their close relationships with biomass and carbon storage [25,33–35,62]. Furthermore, these studies proved that climatic factors in the climate-sensitive models changed with forest types and regions. Carbon storage growth models that include climatic factors may facilitate the effects of future climate change on forest carbon storage.

4.3. Carbon Sequestration Capacity and the Effect of Climate

The dual carbon goal can be achieved by improving carbon sequestration capacity. One of the most economical, feasible and environment-friendly ways to achieve its goal through is making full use of carbon sequestration in terrestrial ecosystems [17]. China's terrestrial ecosystem has a huge carbon sequestration capacity [64]. As the main body of terrestrial ecosystem, forests, especially plantations, play an important role in improving their carbon sequestration capacity. Here, the maximum average increment of carbon storage was taken as the basis for comparison to reflect carbon sequestration capacity. Thus, the carbon sequestration capacity of *Larix*, *P. massoniana*, and *P. tabuliformis* were 1.50, 1.85, and 0.94 t/(ha·a), respectively. The difference in mean carbon growth for different plantation types gradually decreased with the increase in forest age (Table 6 and Figure 7). These results indicate that the carbon sequestration capacity of different plantation types vary greatly, and that each plantation type has a reasonable management cycle. The value of carbon may be considerable in terms of carbon accounting and global climate change. According to the current carbon emission price (dioxide equivalent price USD11 per ton of carbon dioxide equivalent (tCO_2e) [65]), the difference among the three plantations in carbon value per unit area will expand 11 times [65]. It is conceivable that the difference in total value will be greater.

We developed climate-sensitive, variable-parameter carbon storage growth models with a view that a carbon storage model with the climatic factors is better. The average of carbon sequestration capacity of *P. massoniana* and *Larix* plantations reduced by about 4.5% and 3.8%, respectively, when *MAT* decreased by 1 °C. The average of carbon sequestration capacity of *Larix* and *P. tabuliformis* plantations reduced by approximately 6.5% and 3.6%, respectively, when *MAP* decreased by 100 mm. Therefore, climate-adjusted carbon storage estimation is highly important, especially on a large scale. In order to fully develop the maximum production potential in terms of plantation in China, it is vital to coordinate regional development and implement scientific management strategies to fully develop the maximum production potential of plantation in China. It should be noted that the mean growth or carbon sequestration capacity reflected by modelling in this study should be lower than the actual value due to normal tending, cutting, and other business activities that occur in the inventory sample plots of forests resources.

5. Conclusions

Carbon storage growth models for three main species plantations were developed based on the ninth NFI data using a weighted nonlinear regression method. The mean prediction error (*MPE*) of carbon storage growth models was less than 5%, and total relative error (*TRE*) was almost less than 2% for self- and cross-validation, indicating that the carbon storage growth models fit carbon growth well and can objectively reflect the overall mean growth process of the carbon storage in the three tested plantations. Furthermore, the variable parameter carbon storage growth models that included *MAT* and *MAP* performed better than the basic ones.

The carbon sequestration capacity of the three major coniferous plantation types was highest to lowest in *P. massoniana*, *Larix*, and *P. tabuliformis* forests. The age of quantitative maturity for *P. massoniana*, *Larix*, and *P. tabuliformis* were 16a, 24a, and 53a, respectively. Their corresponding maximum average increment of carbon storage was 1.85, 1.50, and 0.94 t/(ha·a), respectively. Based on the maximum mean carbon growth, the carbon sequestration capacity of the *P. massoniana* and *Larix* plantations was approximately 1.97 and 1.60 times that of *P. tabuliformis* plantation, respectively. In addition, with the increase in forest age, the difference in mean carbon growth for different plantation types gradually decreased. Therefore, it is vital to coordinate regional development and implement scientific management strategies to fully develop the maximum production potential of plantations in China.

MAT and *MAP* have different effects on the carbon growth process and carbon sequestration capacity of the three major coniferous plantations. The average carbon sequestration capacity of *P. massoniana* and *Larix* plantations reduced by approximately 4.5% and 3.8%, respectively, when *MAT* decreased by 1 °C. The average carbon sequestration capacity of *Larix* and *P. tabuliformis* plantations reduced by approximately 6.5% and 3.6%, respectively, when *MAP* decreased by 100 mm. In general, the greatest impact of climatic factors on carbon sequestration capacity occurred in the *Larix* plantation, followed by *P. massoniana* and *P. tabuliformis* plantations.

Author Contributions: L.Z. jointly conceived the study with W.Z. (Weisheng Zeng); L.Z., W.Z. (Wentao Zou), G.L. and S.Y. designed the experiments and collected data; L.Z., W.Z. (Weisheng Zeng) and G.L. analyzed the data; L.Z. wrote the manuscript. All authors have read and agreed to the published version of the manuscript.

Funding: This research was funded by the National Science Foundation of China (Grant No. 31901309 and 31770676) and the Fundamental Research Funds for the Central Non-profit Research Institution of CAF (Grant No. CAFYBB2021ZK001).

Institutional Review Board Statement: Not applicable.

Informed Consent Statement: Not applicable.

Data Availability Statement: Not applicable.

Conflicts of Interest: The authors declare no conflict of interest.

References

1. Dixon, R.K.; Brown, S.; Houghton, R.A.; Solomon, A.M.; Trexler, M.C.; Wisniewski, J. Carbon pools and flux of global forest ecosystems. *Science* **1994**, *263*, 185–190. [CrossRef] [PubMed]
2. Pan, Y.; Birdsey, R.; Fang, J.; Houghton, R.; Kauppi, P.; Kurz, W.; Phillips, O.; Shvidenko, A.; Lewis, S.; Canadell, J.; et al. A large and persistent carbon sink in the world's forests. *Science* **2011**, *333*, 988–993. [CrossRef]
3. Liu, Y.; Yu, G.; Wang, Q.; Zhang, Y. Huge carbon sequestration potential in global forests. *J. Resour. Ecol.* **2012**, *3*, 193–201.
4. IPCC (Intergovernmental Panel on Climate Change). *IPCC Guidelines for National Greenhouse Gas Inventories*; Institute for Global Environmental Strategies: Kanagawa, Japan, 2006.
5. IPCC (Intergovernmental Panel on Climate Change). *Climate Change 2014: Mitigation of Climate Change*; Cambridge University Press: Cambridge, UK, 2014.
6. Fang, J.; Yu, G.; Liu, L.; Hu, S.; Chapin, F.S. Climate change, human impacts, and carbon sequestration in China. *Proc. Natl. Acad. Sci. USA* **2018**, *115*, 4015–4020. [CrossRef]
7. Johnston, C.; Buongiorno, J.; Nepal, P.; Prestemon, J.P. From source to sink: Past changes and model projections of carbon sequestration in the global forest sector. *J. For. Econ.* **2019**, *34*, 47–72. [CrossRef]
8. Liu, G.; Fu, B.; Fang, J. Carbon dynamics of Chinese forests and its contribution to global carbon balance. *Acta Ecol. Sin.* **2000**, *20*, 733–740.
9. He, H.; Ge, R.; Ren, X.; Zhang, L.; Chang, Q.; Xu, Q.; Zhou, G.; Xie, Z.; Wang, S.; Wang, H.; et al. Reference carbon cycle dataset for typical Chinese forests via colocated observations and data assimilation. *Sci. Data* **2021**, *8*, 42. [CrossRef] [PubMed]
10. Fang, J.; Guo, Z.; Piao, S.; Chen, A. Terrestrial vegetation carbon sinks in China, 1981–2000. *Sci. China Earth Sci.* **2007**, *50*, 1341–1350. [CrossRef]
11. Fang, J.; Guo, Z.; Hu, H.; Kato, T.; Muraoka, H.; Son, Y. Forest biomass carbon sinks in East Asia, with special reference to the relative contributions of forest expansion and forest growth. *Glob. Chang. Biol.* **2014**, *20*, 2019–2030. [CrossRef]

12. Yu, G.; Li, X.; Wang, Q.; Li, S. Carbon storage and its spatial pattern of terrestrial ecosystem in China. *J. Resour. Ecol.* **2010**, *1*, 97–109.
13. Xu, B.; Guo, Z.; Piao, S.; Fang, J. Biomass carbon stocks in China's forests between 2000 and 2050: A prediction based on forest biomass-age relationships. *Sci. China Life Sci.* **2010**, *53*, 776–783. [CrossRef]
14. Zhu, J.; Hu, H.; Tao, S.; Chi, X.; Li, P.; Jiang, L.; Ji, C.; Zhu, J.; Tang, Z.; Pan, Y.; et al. Carbon stocks and changes of dead organic matter in China's forests. *Nat. Commun.* **2017**, *8*, 151. [CrossRef] [PubMed]
15. Liu, Y.; Yu, G.; Wang, Q.; Zhang, Y.; Xu, Z. Carbon carry capacity and carbon sequestration potential in China based on an integrated analysis of mature forest biomass. *Sci. China Life Sci.* **2014**, *57*, 1218–1229. [CrossRef] [PubMed]
16. State Council. Action Plan on Carbon Emission Peak Pre-2030. 2021. Available online: http://www.gov.cn/zhengce/content/2021-10/26/content_5644984.htm (accessed on 16 March 2022).
17. Fang, J.; Chen, A.; Peng, C.; Zhao, S.; Ci, L. Changes in forest biomass carbon storage in China between 1949 and 1998. *Science* **2001**, *292*, 2320–2322. [CrossRef] [PubMed]
18. Zhao, M.; Zhou, G. Estimation of biomass and net primary productivity of major planted forests in China based on forest inventory data. *For. Ecol. Manag.* **2005**, *207*, 295–313. [CrossRef]
19. Hall, G.; Wiser, S.K.; Allen, R.B.; Beets, P.N.; Goulding, C.J. Strategies to estimate national forest carbon stocks from inventory data: The 1990 New Zealand baseline. *Glob. Chang. Biol.* **2010**, *7*, 389–403. [CrossRef]
20. Li, H.; Lei, Y.; Zeng, W. Forest carbon storage in China estimated using forest inventory data. *Sci. Silvae Sin.* **2011**, *47*, 7–12.
21. Petersson, H.; Holm, S.; Stahl, G.; Akger, D.; Fridman, J.; Lehtonen, A.; Lundstrom, A.; Makipaa, R. Individual tree biomass equations or biomass expansion factors for assessment of carbon stock changes in living biomass-a comparative study. *For. Ecol. Manag.* **2012**, *270*, 78–84. [CrossRef]
22. Mcroberts, R.E.; Westfall, J.A. Effects of uncertainty in model predictions of individual tree volume on large area volume estimates. *For. Sci.* **2014**, *60*, 34–42. [CrossRef]
23. Zhao, H.; Lei, Y.; Fu, L. Biomass and uncertainty estimates of *Pinus massoniana* forest for different site classes in Jiangxi province. *Sci. Silvae Sin.* **2017**, *53*, 81–93.
24. Xue, C.; Xu, Q.; Lin, L.; He, X.; Luo, Y.; Zhao, H.; Cao, L.; Lei, Y. Biomass models with breast height diameter and age for main native tree species in Guangdong province. *Sci. Silvae Sin.* **2019**, *55*, 163–171.
25. Luo, Y.; Wang, X.; Ouyang, Z.; Lu, F.; Tao, J. A review of biomass equations for China's tree species. *Earth Syst. Sci. Data* **2020**, *12*, 21–40. [CrossRef]
26. Zhou, G.; Wang, Y.; Jiang, Y.; Yang, Z. Estimating biomass and net primary production from forest inventory data: A case study of China's *Larix* forests. *For. Ecol. Manag.* **2002**, *69*, 149–157. [CrossRef]
27. Zhang, M.; Wang, G.; Liu, A. Estimation of forest biomass and net primary production for Zhejiang province based on continuous forest resources inventory. *Sci. Silvae Sin.* **2009**, *45*, 13–17.
28. Li, H.; Zhao, P.; Lei, Y.; Zeng, W. Comparison on estimation of wood biomass using forest inventory data. *Sci. Silvae Sin.* **2012**, *48*, 44–52.
29. Li, H.; Ou, Q.; Zhao, J.; Yang, Y.; Quan, F. Effects of model and stand factors on the parameters to carbon accounting at the regional scale—A case study for *Cunninghamia lanceolata*. *Sci. Silvae Sin.* **2017**, *53*, 55–62.
30. Fu, Y.; Lei, Y.; Zeng, W. Uncertainty assessment in regional-scale above ground biomass estimation of Chinese fir. *Sci. Silvae Sin.* **2014**, *50*, 79–86.
31. Guo, Z.; Fang, J.; Pan, Y.; Birdsey, R. Inventory-based estimates of forest biomass carbon stocks in China: A comparison of three methods. *For. Ecol. Manag.* **2010**, *259*, 1225–1231. [CrossRef]
32. Luo, Y.; Wang, X.; Zhang, X.; Ren, Y.; Poorter, H. Variation in biomass expansion factors for China's forests in relation to forest type, climate, and stand development. *Ann. Forest Sci.* **2013**, *70*, 589–599. [CrossRef]
33. Russell, M.B.; Domke, G.M.; Woodall, C.W.; D'Amato, A.W. Comparisons of allometric and climate-derived estimates of tree coarse root carbon stocks in forests of the United States. *Carbon Balance Manag.* **2015**, *10*, 20. [CrossRef]
34. Zeng, W.; Duo, H.; Lei, X.; Chen, X.; Wang, X.; Pu, Y.; Zou, W. Individual tree biomass and growth models sensitive to climate variables for *Larix* spp. in China. *Eur. J. For. Res.* **2017**, *136*, 233–249. [CrossRef]
35. Khan, D.; Muneer, M.A.; Nisa, Z.U.; Shah, S.; Amir, M.; Saeed, S.; Uddin, S.; Munir, M.Z.; Gao, L.; Huang, H. Effect of climatic factors on stem biomass and carbon stock of *Larix gmelinii* and *Betula platyphylla* in Daxing'anling Mountain of Inner Mongolia, China. *Adv. Meteorol.* **2019**, *2019*, 5692574. [CrossRef]
36. Usoltsev, V.A.; Shobairi, S.O.R.; Tsepordey, I.S.; Chasovkikh, V.P. Modelling forest stand biomass and net primary production with the focus on additive models sensitive to climate variables for two-needled pines in Eurasia. *J. Clim. Chang.* **2019**, *5*, 41–49. [CrossRef]
37. Du, X.; Chen, X.; Zeng, W.; Meng, J. A climate-sensitive transition matrix growth model for uneven-aged mixed-species oak forests in North China. *Forestry* **2020**, *94*, 258–277. [CrossRef]
38. He, X.; Lei, X.; Dong, L. How large is the difference in large-scale forest biomass estimations based on new climate-modified stand biomass models? *Ecol. Indic.* **2021**, *126*, 107569. [CrossRef]
39. Guo, H.; Lei, X.; You, L.; Zeng, W.; Lang, P.; Lei, Y. Climate-sensitive diameter distribution models of larch plantations in north and northeast China. *For. Ecol. Manag.* **2022**, *506*, 119947. [CrossRef]

40. National Forestry and Grassland Administration of China. *Report of Forest Resources in China (2014–2018)*; China Forestry Press: Beijing, China, 2019.
41. Zeng, W.; Tomppo, E.; Healey, S.P.; Gadow, K.V. The national forest inventory in China: History-results-international context. *For. Ecosyst.* **2015**, *2*, 23. [CrossRef]
42. *LY/T 2260-2014*; Tree biomass models and related parameters to carbon accounting for *Pinus tabuliformis*. China Standard Press: Beijing, China, 2014.
43. *LY/T 2263-2014*; Tree biomass models and related parameters to carbon accounting for *Pinus massoniana*. China Standard Press: Beijing, China, 2014.
44. *LY/T 2654-2016*; Tree biomass models and related parameters to carbon accounting for *Larix*. China Standard Press: Beijing, China, 2016.
45. Zeng, W.S. Assessment of individual tree above- and below-ground biomass models for 34 tree species in China. In *New Ideas Concerning Science and Technology*; Elangovan, P., Ed.; Book Publisher International: Bhanjipur, India, 2020; Volume 2, pp. 26–37.
46. Bennett, A.C.; Penman, T.D.; Arndt, S.K.; Roxburgh, S.H.; Bennett, L.T. Climate more important than soils for predicting forest biomass at the continental scale. *Ecography* **2020**, *43*, 1692–1705. [CrossRef]
47. Wang, T.; Wang, G.; Innes, J.L.; Seely, B.; Chen, B. ClimateAP: An application for dynamic local downscaling of historical and future climate data in Asia Pacific. *Front. Agric. Sci. Eng.* **2017**, *4*, 448–458. [CrossRef]
48. Ozdemir, E.; Makineci, E.; Yilmaz, E.; Kumbasli, M.; Caliskan, S.; Beskardes, V.; Keten, A.; Zengin, H.; Yilmaz, H. Biomass estimation of individual trees for coppice-originated oak forests. *Eur. J. For. Res.* **2019**, *138*, 623–637. [CrossRef]
49. Xue, C.; Xu, Q.; Lin, L.; He, X.; Cao, L.; Li, H. Biomass dynamic predicting for *Schima superba* in Guangdong based on allometric and theoretical growth equation. *Sci. Silvae Sin.* **2019**, *55*, 86–94.
50. Rohner, B.; Waldner, P.; Lischke, H.; Ferretti, M.; Thürig, E. Predicting individual-tree growth of central European tree species as a function of site, stand, management, nutrient, and climate effects. *Eur. J. For. Res.* **2018**, *137*, 29–44. [CrossRef]
51. Sharma, M.; Zhang, S. Height-diameter models using stand characteristics for *Pinus banksiana* and *Picea mariana*. *Scand. J. For. Res.* **2004**, *19*, 442–451. [CrossRef]
52. Sharma, M.; Subedi, N.; Ter-Mikaelian, M.; Parton, J. Modeling climatic effects on stand height/site index of plantation-grown jack pine and black spruce trees. *For. Sci.* **2015**, *61*, 25–34. [CrossRef]
53. Sharma, M.; Reid, D.E.B. Stand height/site index equations for jack pine and black spruce trees grown in natural stands. *For. Sci.* **2017**, *64*, 33–40. [CrossRef]
54. Newton, P.F.; Amponsah, I.G. Comparative evaluation of five height-diameter models developed for black spruce and jack pine stand-types in terms of goodness-of-fit, lack-of-fit and predictive ability. *For. Ecol. Manag.* **2007**, *247*, 149–166. [CrossRef]
55. Richards, F.J. A flexible growth function for empirical use. *J. Exp. Bot.* **1959**, *10*, 290–301. [CrossRef]
56. Ratkowsky, D.A.; Reedy, T.J. Choosing near-linear parameters in the four-parameter logistic model for radioligand and related assays. *Biometrics* **1986**, *42*, 575–582. [CrossRef]
57. Garcia, O. Comparing and combining stem analysis data and permanent sample plot data in site index models. *For. Sci.* **2005**, *51*, 277–283.
58. Lin, C.; Buongiorno, J. Fixed versus variable-parameter matrix models of forest growth: The case of maple-birch forests. *Ecol. Modell.* **1997**, *99*, 263–274. [CrossRef]
59. Luo, Q.; Zeng, W.; Peng, C. Variable relative tree height curve model and its application in tree volume estimation. *Sci. Silvae Sin.* **1997**, *33*, 202–211.
60. Zeng, W.; Tang, S. Modeling compatible single-tree aboveground biomass equations for masson pine (*Pinus massoniana*) in southern China. *J. For. Res.* **2012**, *23*, 593–598. [CrossRef]
61. Tang, S.Z.; Li, Y.; Fu, L.Y. *Statistical Foundation for Biomathematical Models*, 2nd ed.; Higher Education Press: Beijing, China, 2015.
62. Zhou, R.W.; Li, W.J.; Zhang, Y.P.; Peng, M.C.; Wang, C.Y.; Sha, L.Q.; Liu, Y.T.; Song, Q.H.; Fei, X.H.; Jin, Y.Q.; et al. Responses of the carbon storage and sequestration potential of forest vegetation to temperature increases in Yunnan province, SW China. *Forests* **2018**, *9*, 227. [CrossRef]
63. Fu, L.Y.; Lei, X.D.; Hu, Z.D.; Zeng, W.S.; Tang, S.Z.; Marshall, P.; Cao, L.; Song, X.Y.; Yu, L.; Liang, J.J. Integrating regional climate change into allometric equations for estimating tree aboveground biomass of Masson pine in China. *Ann. For. Sci.* **2017**, *74*, 42. [CrossRef]
64. Wang, J.; Feng, L.; Palmer, P.I.; Yi, L.; Fang, S.; Hartmut, B.; Christopher, W.; Tang, X.; Yang, D.; Liu, L.; et al. Reply to: On the role of atmospheric model transport uncertainty in estimating the Chinese land carbon sink. *Nature* **2022**, *603*, 15–16. [CrossRef] [PubMed]
65. Ramstein, C.S.M.; Dominioni, G.; Ettehad, S.; Lam, L.; Quant, M.; Zhang, J.L.; Mark, L.; Nierop, S.; Berg, T.; Leuschner, P.; et al. *State and Trends of Carbon Pricing 2019*; The World Bank: Washington, DC, USA, 2019.